TKK Dissertations 64
Espoo 2007

HETEROGENEOUS PRECIPITATION AND INTERNAL GETTERING EFFICIENCY OF IRON IN SILICON

Doctoral Dissertation

Antti Haarahiltunen

Helsinki University of Technology
Department of Electrical and Communications Engineering
Micro and Nanosciences Laboratory

TKK Dissertations 64
Espoo 2007

HETEROGENEOUS PRECIPITATION AND INTERNAL GETTERING EFFICIENCY OF IRON IN SILICON

Doctoral Dissertation

Antti Haarahiltunen

Dissertation for the degree of Doctor of Science in Technology to be presented with due permission of the Department of Electrical and Communications Engineering for public examination and debate in Large Seminar Hall of Micronova at Helsinki University of Technology (Espoo, Finland) on the 23rd of March, 2007, at 12 noon.

Helsinki University of Technology
Department of Electrical and Communications Engineering
Micro and Nanosciences Laboratory

Teknillinen korkeakoulu
Sähkö- ja tietoliikennetekniikan osasto
Mikro- ja nanotekniikan laboratorio

Distribution:
Helsinki University of Technology
Department of Electrical and Communications Engineering
Micro and Nanosciences Laboratory
P.O. Box 3500
FI - 02015 TKK
FINLAND
URL: http://www.micronova.fi/units/epg/
Tel. +358-9-451 2322
Fax +358-9-451 5008
E-mail: antti.haarahiltunen@tkk.fi

© 2007 Antti Haarahiltunen

ISBN 978-951-22-8683-6
ISBN 978-951-22-8684-3 (PDF)
ISSN 1795-2239
ISSN 1795-4584 (PDF)
URL: http://lib.tkk.fi/Diss/2007/isbn9789512286843/

TKK-DISS-2273

Otamedia Oy
Espoo 2007

HELSINKI UNIVERSITY OF TECHNOLOGY
P. O. BOX 1000, FI-02015 TKK
http://www.tkk.fi

ABSTRACT OF DOCTORAL DISSERTATION

Author Antti Haarahiltunen

Name of the dissertation

Heterogeneous precipitation and internal gettering efficiency of iron in silicon

Date of manuscript 19.12.2006
Date of the dissertation 23.3.2007

☐ Monograph
☒ Article dissertation (summary + original articles)

Department Electrical and Communications Engineering
Laboratory Micro and Nanosciences Laboratory, Electron Physics Group
Field of research Semiconductor Technology
Opponent(s) D.Sc. (Tech.) Robert Falster
Supervisor (Instructor) Prof. Juha Sinkkonen

Abstract

In this thesis the heterogeneous iron precipitation was studied in silicon using oxide precipitates and related defects as precipitation sites. The motivation of the theoretical work is to find a model which quantitatively describes internal gettering results of iron under various supersaturation levels. The experimental work is used to verify the model.

The results of this thesis indicate that the initial iron concentration level has a major impact on gettering efficiency and a high supersaturation ~0.34 eV is needed before significant nucleation of iron precipitates can occur. The internal gettering of iron at low levels of initial iron concentration ($<1\times10^{12}$ cm^{-3}) is practically impossible to achieve by cooling. The low temperature nucleation anneal is needed to induce a significant number of iron precipitates which then grow and getter iron at higher temperatures. For optimal internal gettering the proper combination of nucleation and growth steps of iron precipitates must be found. The optimal place for two step gettering is after the last high temperature anneal in which all iron precipitates are dissolved, if it is assumed that device performance is mainly determined by the final concentration of metal precipitates and dissolved iron concentration in the device layer.

A model is presented for the heterogeneous precipitation of iron to oxygen-related defects in silicon during thermal processing. In the model we use special growth and dissolution rates, which are inserted into a set of modified Chemical Rate Equations or into the Fokker Planck Equation, to simulate time evolution of iron precipitates. This approach allows us to calculate the size distribution of iron precipitates and the residual iron concentration. By comparing the simulated results with numerous experimental results, it is proved that this model can be used to estimate the internal gettering efficiency of iron under a variety of processing conditions.

Keywords silicon, iron, internal gettering, precipitation, oxide precipitates

ISBN (printed) 978-951-22-8683-6
ISSN (printed) 1795-2239
ISBN (pdf) 978-951-22-8684-3
ISSN (pdf) 1795-4584
ISBN (others)
Number of pages 33+ app. 46
Publisher Helsinki University of Technology, Micro and Nanoscience Laboratory
Print distribution Helsinki University of Technology, Micro and Nanoscience Laboratory

☒ The dissertation can be read at http://lib.tkk.fi/Diss/2007/isbn9789512286843/

TEKNILLINEN KORKEAKOULU PL 1000, 02015 TKK http://www.tkk.fi	VÄITÖSKIRJAN TIIVISTELMÄ
Tekijä Antti Haarahiltunen	
Väitöskirjan nimi Raudan heterogeeninen erkautuminen ja sisäinen getterointiteho piissä	
Käsikirjoituksen jättämispäivämäärä 19.12.2006	Väitöstilaisuuden ajankohta 23.3.2007
☐ Monografia	☒ Yhdistelmäväitöskirja (yhteenveto + erillisartikkelit)

Osasto	Sähkö-ja tietoliikennetekniikan osasto
Laboratorio	Mikro-ja nanotekniikan laboratorio, Elektronifysiikan ryhmä
Tutkimusala	Puolijohdeteknologia
Vastaväittäjä(t)	Tkt Rober Falster
Työn valvoja	Prof. Juha Sinkkonen
(Työn ohjaaja)	

Tiivistelmä

Väitöskirjatyössä tutkittiin raudan heterogeenista erkautumista piissä käyttäen happierkaumia sekä niihin liittyviä virheitä erkautumiskeskuksina. Teoreettisen työn tavoitteena on löytää malli, jolla raudan sisäisen getteroinnin tulokset useilla supersaturaatiotasoilla pystytään kvantitatiivisesti laskemaan. Kokeellisia tuloksia käytettiin mallin tuloksien varmentamiseen.

Tulokset osoittavat, että alkutilanteen rautakonsentraatiolla on erittäin suuri merkitys getterointitehoon ja korkea supersaturaatio ~0.34 eV tarvitaan ennen kuin merkittävää raudan erkautumista voi tapahtua. Pienen alkutilanteen rautakonsentraation ($<1\times10^{12}$ cm^{-3}) tapauksessa sisäistä getterointia ei käytännössä tapahdu jäähdytyksen aikana. Tässä tapauksessa tarvitaan matalan lämpötilan ydintamiskäsittely, jossa syntyy merkittävä määrä rautaerkaumia, jotka voivat kasvaa ja getteroida raudan korkeammassa kasvatus lämpötilassa. Optimaalinen sisäinen getterointi vaati oikeanlaisen yhdistelmän ydintämis- ja kasvatuskäsittelyjä. Kaksivaiheisen getteroinnin optimaalinen paikka on prosessin viimeisen korkean lämpötilan käsittelyn jälkeen, jossa kaikki rautaerkaumat liukenevat, jos oletetaan rautaerkaumien ja liuenneen raudan konsentraation komponenttialueella yksin määräävän komponenttien suorituskyvyn

Raudan heterogeeniselle erkautumiselle happierkaumiin esitetaan malli. Mallissa käytetään erityisiä kasvu- ja liukenemis kertoimia, joiden avulla simuloidaan ajasta riippuvaa raudan erkautumista, käyttäen modifioituja kemiallisia muutosyhtälöitä tai Fokker Planck yhtälöä. Tällä tavalla saadaan laskettua rautaerkaumien kokojakauma ja jäljelle jäänyt liuennut rautakonsentraatio. Vertaamalla simuloituja ja useita kokeellisia tuloksia osoitetaan, että esitettyä mallia voidaan käyttää sisäisen getteroinnin tehon laskentaan hyvinkin erilaisissa prosessointiolosuhteissa.

Asiasanat pii, rauta, erkautuminen, sisäisen getterointi, happierkauma	
ISBN (painettu) 978-951-22-8683-6	ISSN (painettu) 1795-2239
ISBN (pdf) 978-951-22-8684-3	ISSN (pdf) 1795-4584
ISBN (muut)	Sivumäärä 33+ liit. 46
Julkaisija Teknillinen korkeakoulu, Mikro- ja nanotekniikan laboratorio	
Painetun väitöskirjan jakelu Teknillinen korkeakoulu, Mikro- ja nanotekniikan laboratorio	
☒ Luettavissa verkossa osoitteessa http://lib.tkk.fi/Diss/2007/isbn9789512286843/	

Preface

This work was done at HUT during two research projects called *Oxygen precipitation in silicon and its technical applications,* and *Microscopic defect dynamics in silicon*. The projects were funded by the Finnish National Technology Agency, Okmetic Oyj, MAS Oy and VTI Technologies Oy. Financial support from the graduate school of Electrical and Communications Engineering and private organizations (Finnish Technology foundations, Finnish Cultural Foundation) are also acknowledged.

I wish to express my gratitude to my supervisor, professor Juha Sinkkonen, for his advice. I feel deeply honored to have Dr. Robert Falster from MEMC Electronic Materials as my opponent at the defense of the dissertation. I am grateful to pre-examiners Dr. Simo Eränen and Dr. Jari Paloheimo for their evaluation of the thesis.

I want to thank the personnel of the Electron Physics Group for a pleasant working environment. I am grateful for the valuable contribution of my co-authors. I especially want to thank Hele Savin, Marko Yli-Koski and Olli Anttila for motivating me and exchanging ideas about metal precipitation in silicon. I would also like to thank Charlotta Tuovinen for revising my English.

My special thanks belong to my parents, Inkeri and Matti Haarahiltunen, and brother, Olli Haarahiltunen, for giving me self-confidence and support throughout my life.

Finally, I am grateful to my wife, Taina, and my two sons, Otto and Tapani, for their love, encouragement and for keeping my feet on the ground in those moments that I have tended to take my research too seriously.

Espoo, February 2007

Antti Haarahiltunen

Contents

Preface 5

Contents 6

List of publications 7

Author's contribution 8

1 Introduction 9

2 Theory 11

2.1 Heterogeneous precipitation 11
2.2 Segregation to p+ region and effective diffusion 14

3 Results and discussion 17

3.1 Comparison of iron detection methods 17
3.2 Internal gettering 18
3.2.1 Isothermal gettering anneal 18
3.2.2 Slow cooling 21
3.2.3 Nucleation during ramps 23
3.2.4 Gettering dependence on size and density of oxide precipitates 26
3.2.5 Thermal stability of gettering sites 27
3.3 Gettering in process 28

4 Conclusions 30

References 31

List of publications

This thesis consists of an overview and the following selection of the author's publications:

I. A Haarahiltunen, M Yli-Koski, H Väinölä, M Palokangas, E Saarnilehto, and J Sinkkonen, *Experimental study of internal gettering efficiency of iron in silicon,* Physica Scripta **T114,** 91-93 (2004)
II. A. Haarahiltunen, H. Väinölä, M. Yli-Koski, E. Saarnilehto and J. Sinkkonen, *Detection of iron contamination in internally gettered p-type silicon wafers by lifetime measurements,* The Electrochemical Society Proceedings Vol. 05, High purity silicon VIII, Editors: C. L. Claeys, M. Watanabe, R. Falster and P. Stallhofer, p 135-145 (2004).
III. H. Väinölä, A. Haarahiltunen, M. Yli-Koski, E. Saarnilehto and J. Sinkkonen, *Enhancement of internal gettering efficiency of iron by low temperature nucleation,* The Electrochemical Society Proceedings Vol. 05, High purity silicon VIII, Editors: C. L. Claeys, M. Watanabe, R. Falster and P. Stallhofer, p 160-164 (2004).
IV. A. Haarahiltunen, H. Väinölä, O. Anttila, E. Saarnilehto, M. Yli-Koski, J. Storgårds and J. Sinkkonen, *Modeling of heterogeneous precipitation of iron in silicon*, Appl. Phys. Lett. **87** 151908 (2005).
V. A. Haarahiltunen, H. Väinölä, O. Anttila, M. Yli-Koski, and J. Sinkkonen, *Experimental and theoretical study of heterogeneous iron precipitation in silicon,* J. Appl. Phys. **101**, 043507 (2007).
VI. A. Haarahiltunen, H. Väinölä, O. Anttila, M. Yli-Koski and J. Sinkkonen, *Modeling and optimization of internal gettering of iron in silicon*, ECS Transactions Vol. 3 (4), Editors C. L. Claeys, M. Watanabe, R. Falster and P. Stallhofer, 273-284 (2006).

In the overview these publications are referred to by their roman numerals.

Author's contribution

The author Antti Haarahiltunen has developed the mathematical model for heterogeneous iron precipitation in silicon, which is used in Publications IV-VI. He has carried out the simulations presented in Publications I and IV-VI. He has taken part in the designing of experiments in Publications I-V and in Publication II he has also done most of the experimental work. He has written the manuscripts of Publications I-II and IV-VI, and critically revised the manuscript of Publication III.

1 Introduction

Iron is the most investigated metallic impurity in silicon and iron in silicon has been studied extensively over the past 45 years[1]. Over a thousand references related to the topic can be found from review papers[2,3]. The reason for the interest in iron arises mainly from the following facts: i) Iron is a very common metal in process equipment as it is a compound of stainless steel and it is the most common unintentional contamination species in silicon processing. ii) Even a low iron contamination can be detrimental for device yield in the manufacturing of integrated circuits and naturally this makes iron technologically very interesting and important. iii) Iron has easy and sensitive detection methods such as Deep Level Transient Spectroscopy (DLTS), Surface Photo Voltage (SPV) and Microwave Photoconductive Decay (μ-PCD). Therefore iron studies can be done relatively easily.

Iron is detrimental for silicon devices as interstitials iron atoms and their complexes and precipitates introduced deep levels in the bandgap, degrading the lifetime, or generating minority carriers in the depletion region. The incorporation of iron into gate oxide, or precipitation at the Si/SiO_2 interface degrades MOS device yield. In addition to stringent clean room practice the detrimental effect of iron is controlled by the art of gettering[3,4], in which the iron is released from the active area and redistributed to non critical regions of the wafer. Many gettering techniques e.g. internal gettering (IG) and backside damage are based on iron precipitation, i.e. the iron precipitation to gettering sites produces a concentration gradient and iron will diffuse from the active area to gettering sites. This kind of gettering is referred to as relaxation gettering as due to precipitation the gettering is limited by solubility, i.e. the iron concentration is “relaxed” to thermal equilibrium.

A very attractive and popular implementation of this kind of relaxation gettering is internal gettering in which oxide precipitates and related defects in the bulk of wafers serve as gettering/precipitation sites for iron. The advantages of IG are that the gettering sites are relatively close to the active region. IG is possible in double side polished wafers[5,6], and in many cases no additional process step to make gettering sites[i] is needed, although in modern low thermal budget processes this formation of oxide precipitates[5-7] is not guaranteed. However, the IG of iron is still a very practical skill due to lack of quantitative modeling.

In addition to iron precipitation to bulk defects, the important thing in real device processing is competitive gettering, i.e. the iron segregation to highly doped device regions and (heterogeneous) precipitation there.[8] The iron segregation to highly boron doped regions is known to be a very efficient gettering mechanism and it can also be modeled quantitatively.[4,9] However, there is a lack of theoretical work which includes the effect of nucleation of iron precipitates in the device region.

Another interesting field, where the heterogeneous precipitation of iron is important, is multicrystalline silicon solar cells. Multicrystalline silicon includes high concentration of iron

---

[i] Note that this thesis is concentrated on iron precipitation. This means that an optimal way to produce the oxide precipitates has not been looked for, and optimal IG in this thesis always refers to optimal iron precipitation to oxide precipitates.

(10^{14}-10^{15} cm^{-3}), which has precipitated to the grain boundaries and other structural defects.[10,11] Despite of high iron concentration multicrystalline silicon can achieve reasonable operating efficiency as the iron precipitates are less detrimental to solar cell performance than interstitials iron. Additionally, it has been found that small iron precipitates with high density have a larger effect on solar cell performance than the same amount of iron in large precipitates with low density.[10-12] This means that there is a need for modeling which can be used for the optimization of the size distribution of iron precipitates.

The studies for this thesis were started by experimental studies (Publications I, II and III). In Publication II a comprehensive comparison between iron detection methods particularly in internally gettered silicon wafers was also done. During these experimental works it was noticed that the gettering results are far from the predictions of a widely used model for heterogeneous iron precipitation as shown in Publication I. The existing model was unable to even qualitatively explain the experimental results presented in Publication III. The work was then extended to develop the modeling of heterogeneous iron precipitation in silicon (Publication IV). In Publication V new experimental results of iron precipitation were presented and analyzed using the proposed model. In Publication VI the modeling was extended to situations which also include competitive gettering. However, in this thesis the theory is presented first and it is followed by the results and a discussion.

2 Theory

As experimental process optimization for the impurity gettering is expensive and time consuming, several theoretical papers[13-19] discuss modeling of iron gettering. In these papers the iron precipitation to oxide precipitates is usually modeled by Ham's law[20] and it is further assumed that all oxide precipitates are effective (active) gettering sites, i.e. all of the oxide precipitates contain iron precipitate(s). It is experimentally confirmed that using Ham's law the iron precipitation can be described at very high supersaturation.[13,21] The simulations greatly overestimate the gettering efficiency of slowly cooled samples (Publication I), when Ham's law and oxide precipitate density are used. A better agreement between simulation and experimental results was achieved by using a significantly lower effective gettering site density than oxide precipitates density as shown in Publication I. This means that nucleation of iron precipitates must be taken into account and the number of effective gettering sites might be only a small portion[13,22,23] of the total oxide precipitate density. In this chapter a model is presented (Publications IV and V) which includes the nucleation and properly takes into account the effect of the supersaturation level. The models for solubility[2,3,8,24] and diffusivity[9,25] of iron as a function of boron concentration are reviewed as they are used in competitive gettering simulations in Publication VI. In the simulations in which the denuded zone, DZ, (or oxide precipitate free zone) or the boron doped layer is included, diffusion and segregation are calculated by an algorithm which is described in detail in Ref. 14.

2.1 Heterogeneous precipitation

Classical nucleation theory is based on the assumption that a precipitate can grow or dissolve only by one atom at a time. Such a cluster evolution is described by the Chemical Rate Equations (CRE)

$$\frac{\partial f_n}{\partial t} = I_n - I_{n+1} \qquad n = 0,1,... \quad , \tag{1}$$

where n is the number of iron atoms and f_n is the density of heterogeneous precipitation sites containing n atoms of precipitated iron. The flux from size n-1 to size n is

$$I_n = g_{n-1} f_{n-1} - d_n f_n \quad , \tag{2}$$

where g_n and d_n are growth and dissolution rates, respectively.

Conventionally, the CRE are used to model homogeneous nucleation. In our model the idea is that we simulate how the heterogeneous precipitation sites attract the iron atoms. That also justifies the use of Eq. (1) to model precipitates of all sizes. In addition, in our model the index n starts from zero in contrast to the modeling of the homogeneous nucleation and f_0 refers to the density of gettering sites, which do not contain iron, i.e., they have not yet become effective precipitation sites for iron. The density of effective precipitation sites and the concentration of precipitated iron can be calculated from the simulated size distribution function. The rate of change in the interstitial iron concentration can be calculated from

$$\frac{\partial C_{\mathrm{Fe}}}{\partial t} = -\sum_{n=0} I_n \ , \qquad (3)$$

where C_{Fe} is the interstitial iron concentration, or from

$$\frac{\partial C_{\mathrm{Fe}}}{\partial t} = -\frac{\partial}{\partial t}\sum_{n=1} n f_n \ . \qquad (4)$$

It is reasonable to assume that the iron concentration at the interface of a gettering site is in thermodynamical equilibrium with the iron precipitate, i.e. the growth of iron precipitates is a diffusion limited process. Making the further assumptions that this equilibrium interface concentration is equal to the solid solubility of iron and all of the oxide precipitates are active gettering sites, the change in the interstitial iron concentration due to heterogeneous precipitation of iron can be calculated as suggested by Tan et al. [16]

$$\frac{\partial C_{\mathrm{Fe}}}{\partial t} = -4\pi r_{ox} N_{ox} D\left(C_{\mathrm{Fe}} - C_S\right) \qquad , \qquad (5)$$

where N_{ox} is the total density of oxide precipitates, r_{ox} is the average radius of the oxide precipitates, D is the diffusion constant of iron, and C_S is the solid solubility of iron in silicon. Eq. (5) can be obtained from Ham's diffusion limited precipitation law for fixed radius[17,20], thus, we refer to Eq. (5) as Ham's law. We presume that the equilibrium iron concentration at the interface depends on the number of iron atoms precipitated to the gettering site. This assumption can be justified using general nucleation theory, in which the equilibrium concentration depends on the size of the nucleus[26]. For simplicity we assume that the local equilibrium concentration has the form

$$C_{eq} = C_S \exp\left(\frac{E_a}{kTn^{1/2}}\right) \qquad , \qquad (6)$$

where $E_a/n^{1/2}$ describes the fact that iron has a higher chemical potential in a small cluster than in a large cluster. C_S is the equilibrium concentration at the interface of a very large iron precipitate, k is the Bolzmann constant and T is the temperature. Note that it is assumed that the morphology of iron precipitates is disk-shaped and the change in Gibb's free energy is approximately[27]

$$\Delta G(n) = -nkT\ln\left(\frac{C_{\mathrm{Fe}}}{C_S}\right) + 2E_a n^{1/2} \ . \qquad (7)$$

E_a is a fitting parameter which is related to the surface energy and includes also the possible effect of the strain[28-30] and the morphology of oxide precipitates as well as the charge state of iron[31] which all have their own contributions to the iron precipitation behavior.

The experiments[13,21] suggest that iron is apparently captured by a surface, which is larger than the surface of the iron precipitate itself. However, we do not know for sure whether it is the

oxide precipitates or secondary defects associated with oxide precipitates that act as the gettering sites for iron. When modeling the internal gettering, we choose the total density and the average radius of the oxide precipitates to characterize gettering sites as these seem to have correct magnitudes. Consequently, we obtain the growth and dissolution rates for heterogeneous iron precipitation from Eq. (5) by replacing the solid solubility of iron with the size dependent equilibrium concentration C_{eq}[32]

$$g_n = 4\pi r_{ox} D C_{\mathrm{Fe}} \text{ and } d_n = 4\pi r_{ox} D C_{eq} . \qquad (8)$$

Using Eqs. (2,4 and 8) it can be easily shown that our model reduces to Eq. (5) at high supersaturation , i.e. when $C_{\mathrm{Fe}} >> C_{eq}$ at all n. This can be seen by writing out Eq. (3)

$$\frac{\partial C_{\mathrm{Fe}}}{\partial t} = -4\pi r_{ox} D C_{\mathrm{Fe}} (f_0 + f_1 ...) + 4\pi r_{ox} D (f_1 C_{eq}(1) + f_2 C_{eq}(2) + ..) \qquad (9)$$

At high supersaturation Eq. (9) reduces to Ham's law which is

$$\frac{\partial C_{\mathrm{Fe}}}{\partial t} \approx -4\pi r_{ox} N_{ox} D C_{\mathrm{Fe}} \qquad , \qquad (10)$$

where

$$N_{ox} = \sum_{0} f_n . \qquad (11)$$

Generally, after nucleation, our model reduces to Eq. (5) with a revision: N_{ox} is replaced by the density of effective precipitation sites

$$N_{eff} \approx \sum_{1} f_n . \qquad (12)$$

Experiments also show that Eq. (5) is approximately valid for iron at very high supersaturation[13,21], for example, as the temperature is around 200 ^{o}C and the iron contamination level is around 1×10^{13} cm^{-3}

The Chemical Rate Equations can be solved using the selected grid point method as we have done in Publication IV. This solution is rather time consuming, and thus we used the Fokker-Planck Equation (FPE),

$$\frac{\partial f(n,t)}{\partial t} = \frac{\partial}{\partial n}\left(-A(n,t) f(n,t) + B(n,t) \frac{\partial f(n,t)}{\partial n} \right), \qquad (13)$$

where

$$A(n,t) = g(n,t) - d(n,t)$$
$$B(n,t) = \frac{g(n,t) + d(n,t)}{2}, \quad (14)$$

to simulate evolution of size distribution in Publications V and VI.

The practical numerical solution of the FPE, which is unconditionally stable so the larger time-steps are allowed, is given in Ref. 33. The solution of the FPE requires boundary condition at size one, which is set to

$$f(1,t) = P_1 f(0,t) \exp\left(\frac{-\Delta G(1)}{kT}\right) \quad (15)$$

which is actually the size distribution function for a quasi-equilibrium state in an ideal heterogeneous nucleation process adjusted with a fitting parameter P_1. [34]

In simulation, after finding proper fitting parameters E_a and P_1, the input parameters are the density and radius of oxide precipitates, which in practice can be measured or estimated by various methods as discussed in Publication V. In the beginning of the simulation, it is assumed that no iron precipitates (effective gettering sites) exist, and f_0 is set to equal to the density of oxide precipitates. It is important to realize that in this case the gettering can occur only after the formation of a significant number of active gettering sites, i.e. after nucleation. Whereas, in Ham's law (Eq. (5)) it is assumed, that iron diffusion to all oxide precipitates take place immediately, when the iron concentration exceeds the solubility.

2.2 Segregation to p+ region and effective diffusion

The total iron concentration in boron doped silicon is the sum of neutral iron, positively charged iron, and the Fe-B pairs. The positively charged iron concentration, Fe^+, is given by[24]

$$\mathrm{Fe}^+ = \frac{1}{2}\mathrm{Fe_i} \exp\left(\frac{E_D - E_F}{kT}\right), \quad (16)$$

where Fe_i is the concentration of neutral iron in intrinsic silicon, E_D is the iron donor level, and E_F is the Fermi level in the silicon band gap with respect to the valence band edge. Eq. (16) applies to either intrinsic or doped material. The Fe-B pair concentration is[35,36]

$$(\mathrm{Fe\text{-}B})_{\mathrm{pair}} = \mathrm{Fe}^+ \frac{4 \times \mathrm{B}^-}{\left[\frac{5 \times 10^{22}}{cm^{-3}}\right]} \exp\left(\frac{0.65eV}{kT}\right), \quad [\mathrm{cm}^{-3}] \quad (17)$$

where B^- is the concentration (cm^{-3}) of negatively charged boron atoms.

It is easy to understand that, if you compare the same total iron concentration in intrinsic silicon and in boron doped silicon, in latter case there is much less neutral iron. In the solubility model the maximum concentration of neutral iron is expected to remain constant, i.e. the solubility of iron in boron doped silicon is enhanced as in the same concentration of neutral iron there is additionally positively charged iron and iron boron pairs. The segregation coefficient, which is defined as the ratio of solubilities, is then[24]

$$k_{Seg}(\mathrm{B}) = \frac{C_S(\mathrm{B})}{\mathrm{C}_S} = \left[\frac{1}{1+\frac{1}{2}\exp\left(\frac{E_D - E_i}{kT}\right)}\right] \times \left[\left[1+\frac{1}{2}\exp\left(\frac{E_D - E_F}{kT}\right)\right] \times \left[1+\frac{4\times \mathrm{B}^-}{\left[\frac{5\times 10^{22}}{cm^{-3}}\right]}\exp\left(\frac{0.65eV}{kT}\right)\right]\right], \quad (18)$$

where $C_S(\mathrm{B})$ is iron solubility in boron doped silicon and E_i is the Fermi level in intrinsic silicon.

The effective diffusivity of iron in boron-doped materials is[9]

$$D = f \times D^{eff}(\mathrm{Fe}^+) + (1-f)\times D(\mathrm{Fe}), \quad (19)$$

where f is the fraction of ionized iron. The effect of trapping of Fe^+ by boron on the effective diffusivity of positively charged iron can be calculated[9]

$$D^{eff}(\mathrm{Fe}^+) = \frac{D(\mathrm{Fe}^+)}{1+4\pi\,\tau_{diss} D(\mathrm{Fe}^+) R_C \mathrm{B}^-}, \quad (20)$$

where $D(\mathrm{Fe}^+)$ is the diffusivity of positive interstitial iron without pairing with boron, τ_{diss} is the dissociation time constant of iron-boron pairs and R_C is the capture radius of iron-boron pairs. Although the positively charged and neutral iron may have different diffusion constants, the single line could be fitted through the literature data of iron diffusivity[2], thus it seems reasonable to use

$$D(\mathrm{Fe}) = D(\mathrm{Fe}^+) = 1\times 10^{-3} \times \exp\left(\frac{-0.67eV}{kT}\right) \ [\mathrm{cm}^2/\mathrm{s}]. \quad (21)$$

The dissociation time constant of iron-boron pairs is[25]

$$\tau_{diss} = (9.35\times 10^{-16})\times \exp\left(\frac{1.40eV}{kT}\right). \qquad [\mathrm{s}] \quad (22)$$

The capture radius is obtained by solving the following equation[2]

$$kT = \frac{q^2}{4\pi\,\varepsilon\,\varepsilon_0 R_C} \exp\left[-R_C \Big/ \left(\frac{\varepsilon\,\varepsilon_0 kT}{q^2 p} \right)^{1/2} \right], \tag{23}$$

where p is the hole concentration.

The temperature-dependent position of the iron donor level was calculated using a step like function, which provides the best fit to available experimental data[8]

$$\begin{aligned} E_D - E_V &= \left(2.956 \times 10^{-5} \times \left[\frac{T}{K} \right] + 0.38 \right) eV, T \le 1015K \\ E_D - E_V &= \left(1.6522 - 1.224 \times 10^{-3} \times \left[\frac{T}{K} \right] \right) eV, 1015K < T \le 1350K, \\ E_D - E_V &= 0, T > 1350K \end{aligned} \tag{24}$$

where E_V is the valence band edge.

3 Results and discussion

The iron concentration can be measured with a very good detection limit ~10^{10} cm^{-3} by DLTS. However, DLTS is hardly suitable for large area detection, i.e. wafer mapping, as an additional contact preparation is needed. In experiments the DLTS drawbacks are also low throughput of samples and wafers must be broken for measurement. Thus it would be beneficial to use lifetime methods to make iron concentration measurements. In Publication II it was studied how suitable lifetime methods are for the iron detection from internally gettered wafers and these results are presented first. Next the proposed model from Publications IV and V is used to analyze the experimental results of the IG of Publication V and model parameters are fitted. The experimental results of slow cooling from Publication I and II, optimization of IG from Publication III and thermal stability of gettering sites from the publication of Zhang et al.[37] are discussed on the basis of modeling. The experimental details can be found in Publications I-V and only essential parts are repeated in this chapter.

3.1 Comparison of iron detection methods

The wafers were intentionally iron contaminated to a level of about 1-2×13 cm^{-3}. Different kinds of gettering treatments were applied in Publication II to obtain a wide range of dissolved iron concentrations. The results indicate that an iron concentration down to 1×10^{11} cm^{-3} can be quantitatively measured in internally gettered wafers by lifetime methods. In internally gettered wafers μ-PCD has a lower detection limit for iron than SPV but in both cases the detection limit depends on the internal gettering process. The oxide precipitates are stronger lifetime killers at low injection levels[38] which explains the lower detection limit of μ-PCD.

The reference measurements were done by DLTS. The correlation between measurements is shown in Fig. 1. Based on results shown in Fig. 1 it was decided to use μ-PCD as the main detection method in Publication V. DLTS measurements were used only in cases when iron detection by μ-PCD was not reliable.

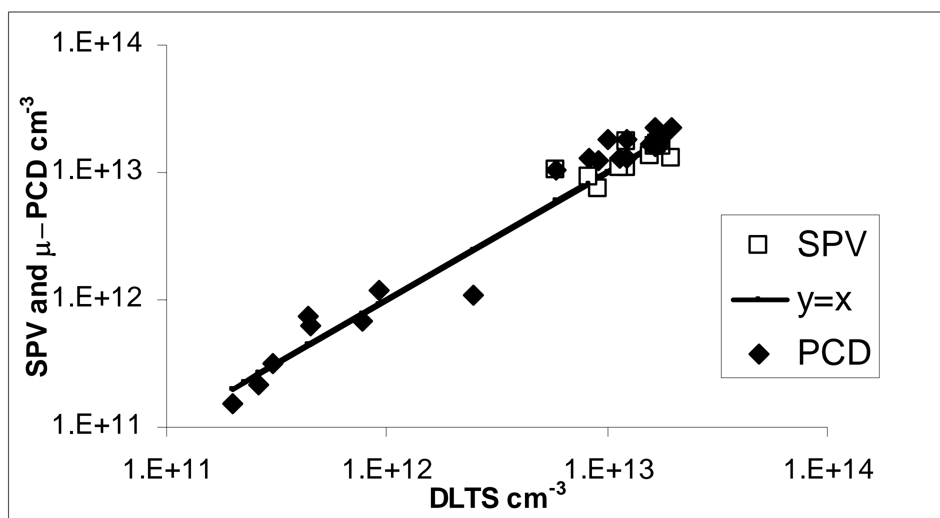

FIG. 1. The comparison between DLTS, SPV and μ-PCD results.

3.2 Internal gettering

3.2.1 Isothermal gettering anneal

In publication V iron precipitation was studied by using three different initial iron contamination levels: 5×10^{12} cm^{-3}, 2×10^{13} cm^{-3}, and 8×10^{13} cm^{-3}. The oxide precipitate density was about 1×10 cm^{-3} and the size was about 80 nm measured by defect etching and Transmission Electron Microscopy (TEM), respectively. Iron was then gettered by a 30 minute isothermal anneal in a temperature range of 300 – 800 °C. Before each gettering anneal, the wafers were annealed for 30 minutes at the contamination temperature to dissolve the possible iron nuclei that are formed during contamination. The wafers were then cooled at the rate of 50 ºC/min to the gettering temperature. After the gettering anneal, the wafers were cooled to room temperature at the rate of 100 ºC/min. In other words, the outline of the gettering annealing is as follows: 30 min dissolution anneal → cooling 50 ºC/min → 30min@200-800ºC → cooling 100 ºC/min to RT. More details of the experiments can be found in Publication V.

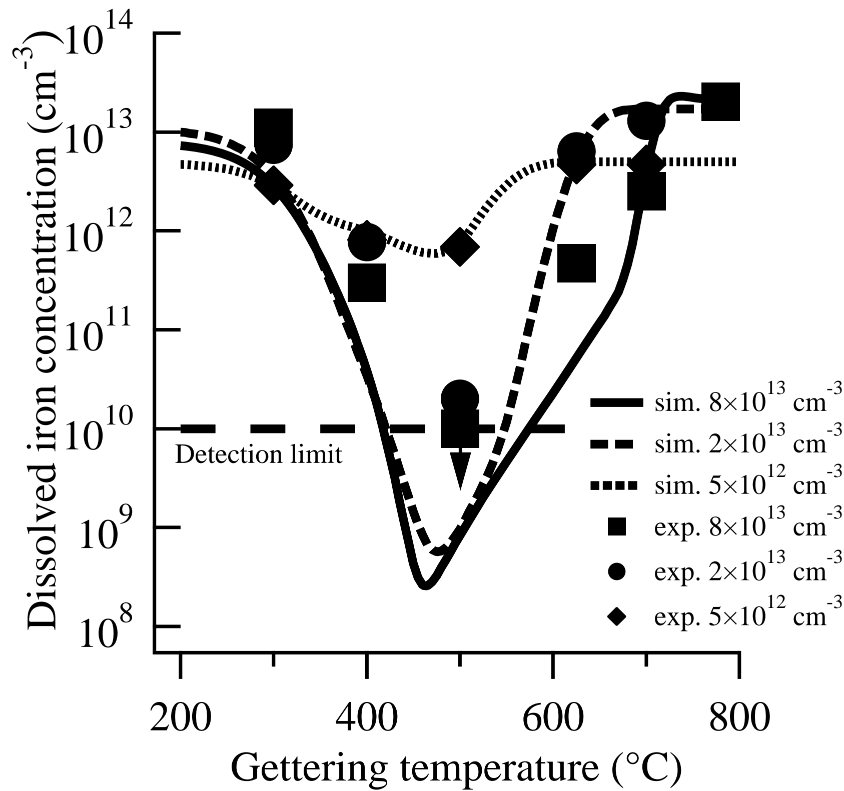

FIG. 2. The comparison of simulated (lines) and experimental results (symbols) of remaining dissolved iron concentration measured after a 30 min anneal in certain temperatures. The initial iron concentrations were 8×10^{13} (square; solid line), 2×10^{13} (circle, dashed line) and 5×10^{12} cm^{-3} (diamond, dotted line). Figure is the same as in Publication V (Reprinted with permission from American Institute of Physics).

The experimental results are shown by symbols in Fig. 2. At 300ºC, the gettering is limited by diffusion and almost no gettering takes place in any wafer. More interesting observations can be made at higher temperatures. The dissolved iron concentration depends strongly on the initial iron concentration: The higher the initial iron concentration, the less iron is measured after gettering. Note that at 500 ºC the highest initial contamination level is gettered below our detection limit of 1×10^{10} cm^{-3}. Therefore, the level of supersaturation, kT*ln(C_{Fe}/C_S), evidently plays a significant role in the final gettering efficiency. The effect of the supersaturation level is further supported by the observation that a rather high supersaturation is required before precipitation occurs at all. In Publication IV we suggested that the critical supersaturation level is about 0.34 eV. Actually, this can be used as rule of thumb when considering whether the iron precipitates or not as shown in Table I, which compares the calculated supersaturation levels to the observed gettering at different temperatures. This is quite surprising as also the diffusivity, density and radius of oxide precipitates, i.e. the timescale of the experiment, affects the observed gettering. However, the critical supersaturation level was estimated from experimental results of slowly cooled samples with a high density of gettering sites and that is why the timescale might be good when considered the above 30 min isothermal gettering anneal also with high density of gettering sites.

Table 1. Comparison of calculated supersaturation and gettering. Bolding indicates experimentally observed gettering.

Temperature (°C)	Supersaturation (eV) 8×10^{13} cm^{-3}	Supersaturation (eV) 2×10^{13} cm^{-3}	Supersaturation (eV) 5×10^{12} cm^{-3}
300	**1,11**	**1,04**	**0,97**
400	**0,93**	**0,85**	**0,77**
550	**0,67**	**0,58**	**0,48**
625	**0,54**	**0,44**	0,33
700	**0,41**	**0,30***	0,18
780	**0,28***	0,15**	0,02**

*some gettering occurs during cooling down, ** no experimental results

The corresponding simulation results are shown by lines also in Fig 2. In our simulations we use $C_S=4.3\times10^{22}\exp(-2.10\text{eV}/kT)$ cm^{-3} Ref. (39), $D=1\times10^{-3}\exp(-0.67\text{eV}/kT)$ cm^2/s Ref. (2) and gettering site parameters: $N_{ox}=1\times10^{10}$ cm^{-3} and r_{ox}=40 nm. The fitting parameters of the model were obtained by the least square method using experimental results of a 30 min isothermal anneal. Fitted parameters are $P_1=1\times10^4$, $E_a=(1.015\times10^{-4}[T/K]+0.8033)$ *eV*, $T<773$ K and $E_a=(6.038T\times10^{-4}[T/K]+0.4150)$eV, T≥773 K. With these parameters the experimental results can be fitted quite well, as shown in Fig. 2.

The fitting parameter P_1 should in the ideal case be one. In our case, it is much larger, which might indicate that each oxide precipitate contains several possible nucleation sites. If we assume that the number of possible nucleation site in our case is equal to the fitted P_1, we can estimate that the density of state in the surface of the oxide precipitate is 5×10^{13} cm^{-2}. If it is estimated from the density of the silicon atom and the lattice constant of silicon, it should be about 1.4×10^{15} cm^{-2} .[18]

The fitting parameter E_a equals a surface energy between 1.8×10^{14} to 3.6×10^{13} cm^{-3}- $eVcm^{-2}$ if it assumed that the thickness of the disk is between 1 and 5 nm. The estimation of surface energy is done using equation 5 from Ref. 27 and using 3.9×10^{-23} cm^{-3} [40] as the iron precipitate volume per iron atom. Further, it is assumed that the thickness of the disk is small compared to its radius. Nakamure et al. [18] used the value 6.9×10^{13} $eVcm^{-2}$ and Brown et al. [41] used the value 3.5×10^{14} $eVcm^{-2}$ in their calculations. The temperature dependency of E_a is understandable if the iron precipitate has several stable silicides.[29.42]

The results of Fig. 2 can be plotted as a s-curve which is typical e.g. for oxygen precipitation[34,43]. In Fig. 3 the results of gettering at temperatures of 500, 625 and 700 ºC are shown. Fig. 3 clearly points out that when the initial supersaturation is above some threshold nearly all iron precipitates. This is well captured by the proposed model although there remains some difference in the final dissolved iron concentrations (Fig. 2).

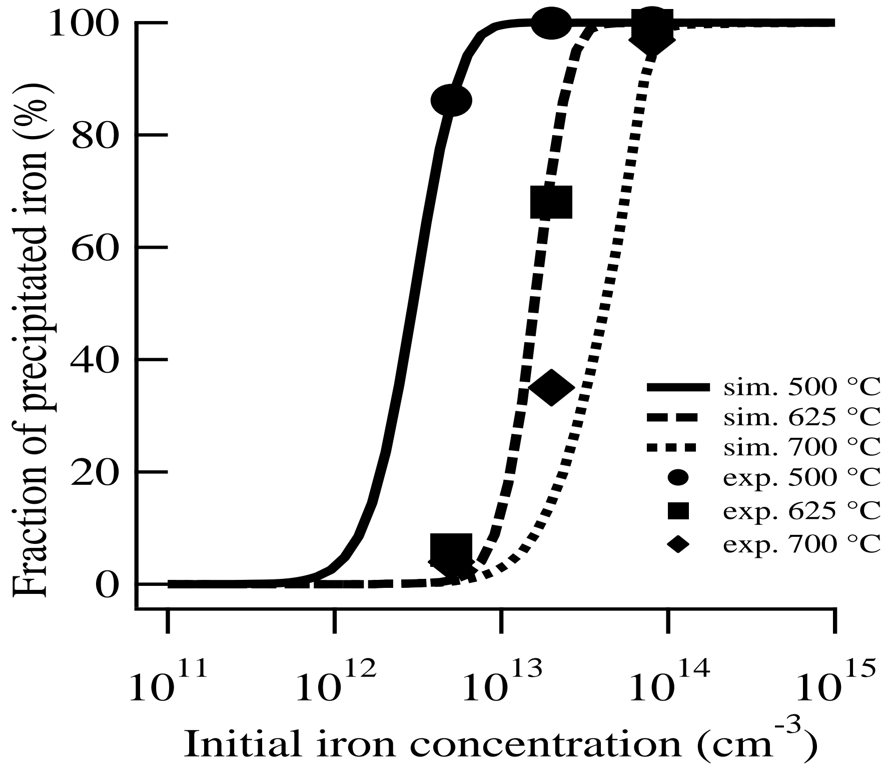

FIG. 3. Simulated and experimental s-curve of iron precipitation at 700 ºC (diamond, dotted line), 625 ºC (square, dashed line) and 500 ºC (circle, solid line). The simulations include programmed ramps of the furnace. Figure is the same as in Publication V (Reprinted with permission from American Institute of Physics).

As an example the simulated size distributions after gettering at 700 ºC is shown in Fig. 4. It can be seen that only the highest initial iron concentration has a peak at the large size. The average size is 4.4×10^{5}, which equals a disk radius between 33 and 73 nm with a thickness between 5 and 1 nm. The reason for this peak is nucleation and growth during the 30 minute anneal at 700 ºC. There is no such peak at lower iron concentrations as there is no significant

nucleation at 700 ºC. The "tail" at the lower size is actually produced during the cooling down period. At the contamination level 5×10^{12} cm^{-3} the simulation actually predicts non-detectable iron precipitation as the iron precipitates are so small. This is exactly what is observed experimentally. The important thing here is to realize, that even if the iron precipitation cannot be detected by measuring loss of interstitials iron, the tail has a great impact on further processing. Actually, these kinds of tails are the reason for the dissolution anneal before each of the isothermal gettering anneals. Without dissolution the small iron precipitates produced during contamination could dominate the experimental results (Publication III).

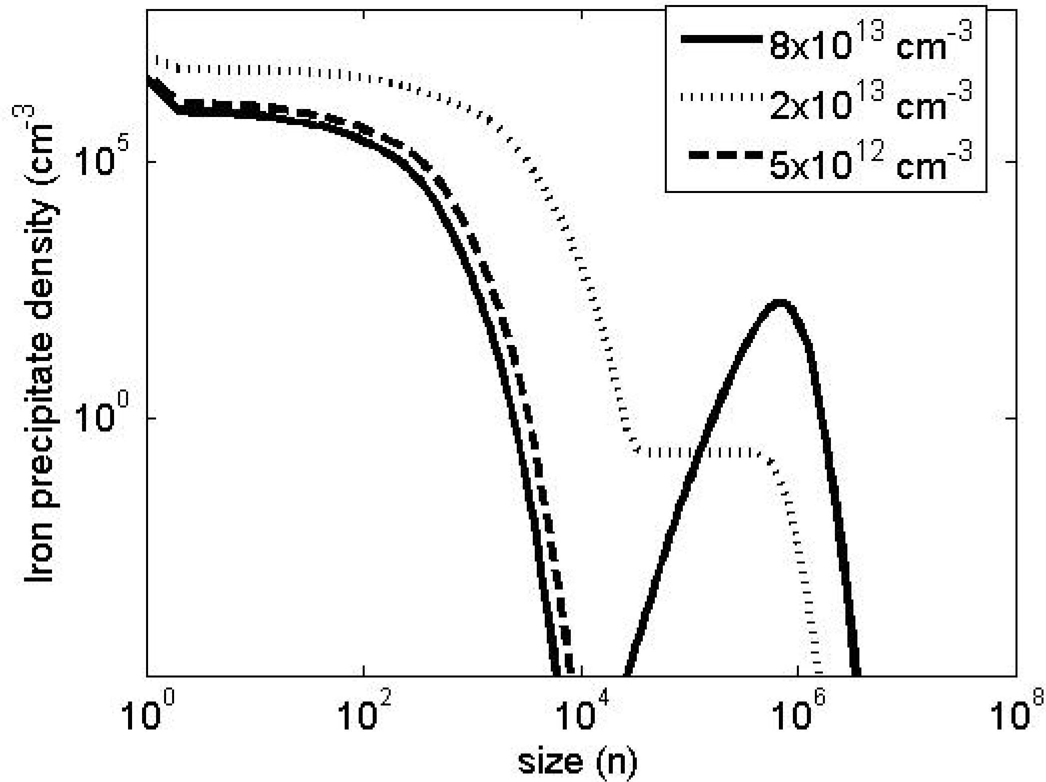

Fig. 4. Simulated size distributions of iron precipitates after gettering anneal at 700 ºC. The initial contamination level is 8×10^{13} cm^{-3} (solid line), 2×10^{13} cm^{-3} (dotted line) and 5×10^{12} cm^{-3} (dashed line). The simulation includes ramps.

3.2.2 Slow cooling

Traditionally, it is assumed that efficient internal gettering occurs during cooling after a high temperature process. The efficiency of this kind of gettering was studied in Publications I and II. Fig. 5 shows the experimental and simulation results of slow cooling (2 ^{o}C/min) from 850 ^{o}C to different pull out temperatures with initial iron concentrations of 1.3×10^{13} and 2.2×10^{13} cm^{-3}. In these simulations the DZ is 50 µm, the radius of the oxide precipitate is 76 nm and the oxide precipitate density in bulk is 2×10^{10} cm^{-3}. In the DZ the oxide precipitate density and radius are set to 5×10^{8} cm^{-3} and 0.2 nm, respectively, as estimated by Hieslmaier et al..[13]

Hieslmair et al.[13] have observed experimentally that only some of the oxide precipitates serve as iron gettering sites at high temperatures or, as they claimed, that only some portion of the

oxide precipitates surfaces are active. In publication VI we showed that their results are strongly affected by nucleation during quenching and loading. The simulated iron precipitation site density is about 7.7×10^{7} cm^{-3} after cooling the wafer to 600 ^{o}C, i.e., more than three orders of magnitude smaller than the reported oxide precipitate density (publication IV).

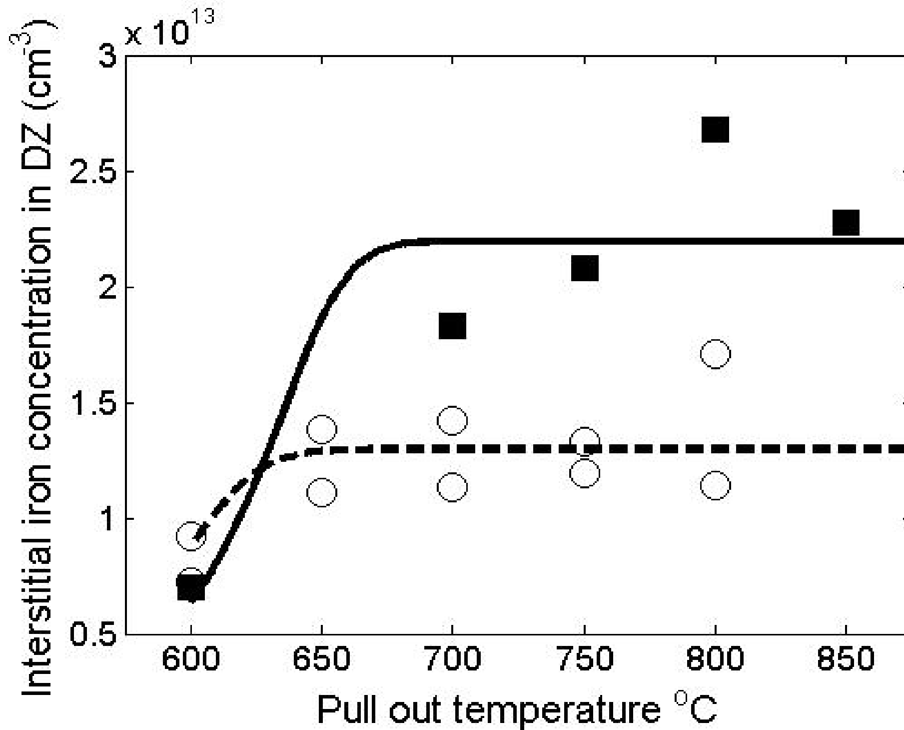

Fig. 5. Experimental results of slow cooling (2 ^{o}C/min) from 850 ^{o}C to pull out temperature (squares Publication I) and (open circles Publication II). In the simulated results the initial iron concentration is 2.2×10^{13} cm^{-3} (solid line) or 1.3×10^{13} cm^{-3} (dashed line). Figure is the same as in Publication VI (Reproduced by permission of ECS – Electrochemical Society).

It is interesting to analyze gettering efficiency as a function of cooling rate and initial iron concentration level as the results of Fig. 2-3 indicate that the gettering efficiency is strongly dependent on the initial iron concentration. In these simulations the DZ is set to 20 μm and other parameters are the same as in the simulation presented in the previous figure. The simulation results are presented in Fig. 6. We may conclude that only the high initial iron concentrations, above 1×10^{13} cm^{-3}, can be gettered simply by pulling out of the furnace, i.e. high cooling rate >100 K/min. The gettering of low level iron concentrations, below 1×10^{12} cm^{-3}, is impossible at any realistic cooling rates. This is because a sufficiently high supersaturation level and diffusivity are not reached simultaneously under these processing conditions.

Aoki et al.[39] observed significant gettering during pulling out at a contamination level of about 4×10^{14} cm^{-3} whereas no gettering was observed at a contamination level of 4×10^{12} cm^{-3}. Palokangas[44] also observed that that gettering of iron at the contamination level of 10^{11} cm^{-3} is not possible even by extremely slow cooling (0.2 K/min) to 500 ^{o}C. These results are clearly in agreement with the simulation results shown in Fig. 6.

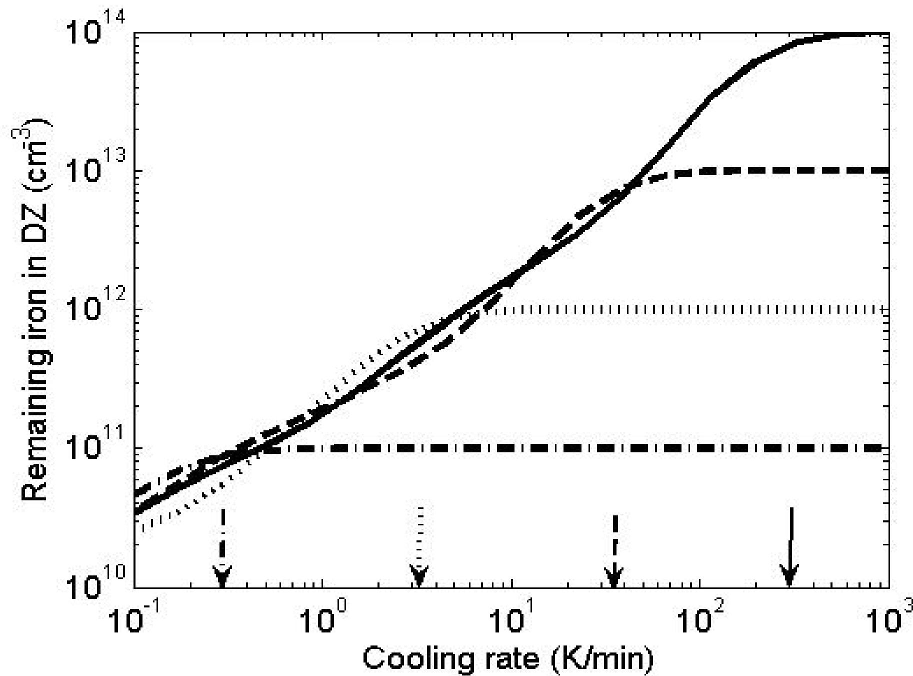

FIG. 6. The remaining iron in the DZ versus the linear cooling rate. The cooling is done from 1000 to 200 ºC. The initial iron concentrations were 1×10^{14} (solid line), 1×10^{13} (dashed line), 1×10^{12} (dotted line) and 1×10^{11} cm^{-3} (dashed-dotted line). Arrows mark the cooling rates where gettering starts at each initial iron concentration. Figure is the same as in Publication VI (Reproduced by permission of ECS – Electrochemical Society).

3.2.3 Nucleation during ramps

The problems in gettering of low level iron concentrations by cooling might be overcome by using a low temperature nucleation anneal as shown in Publication III. In our experiments in Publication III the wafers were divided into two different gettering treatments: i) In the first treatment the wafers were annealed at 900 ^{o}C and then slowly cooled to 700 ^{o}C where the isothermal gettering anneal was performed. ii) In the second treatment the wafers were pulled out directly from 900 ^{o}C, air cooled to RT, loaded again to 700 ^{o}C and annealed further for different times. More details of the experiments can be found in Publication III.

As shown in Fig. 7 the ramp to RT has a drastic effect on the iron precipitation behavior at 700 ^{o}C. The simulation agrees with the experiments in that no gettering occurs when wafers are annealed at 700 ^{o}C after cooling from 900 ^{o}C. In these simulations the DZ is 50 µm, the radius of the oxide precipitate is 76 nm and the oxide precipitate density in bulk is 2×10^{10} cm^{-3}. The RT step is simulated as quenching. The simulation predicts a too fast iron precipitation when the RT step is included, however, in the experiments the cooling was not quenching.

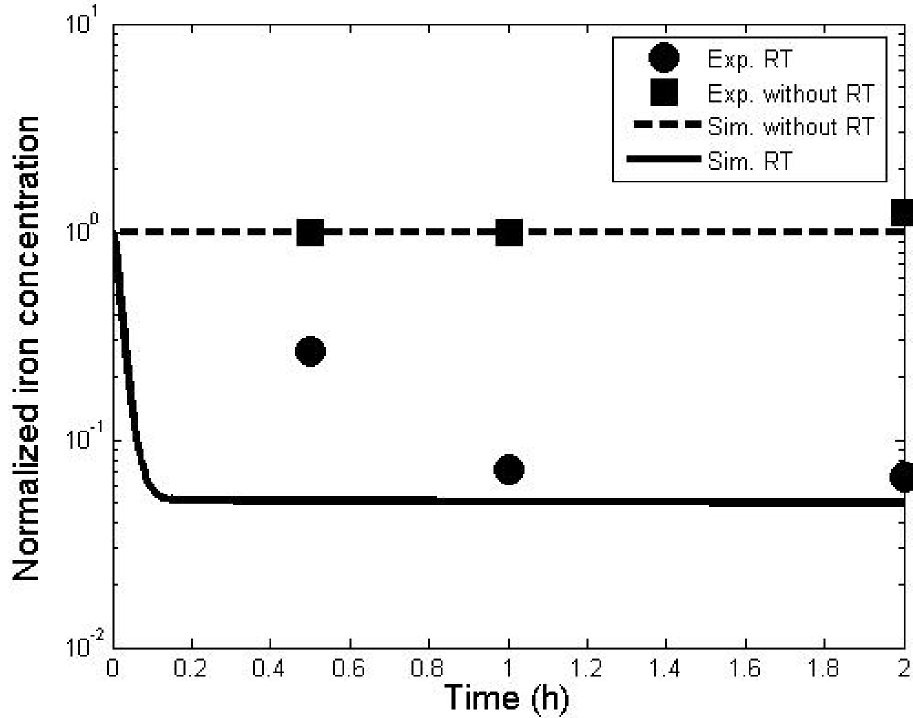

FIG. 7. The interstitial iron concentration (in the DZ) dependence on annealing time at 700 °C. The squares are our experimental results from Publication III without a room temperature step and the circles are experimental results when the RT step is included in the process. The simulated results without the RT step (dashed line) and with the RT step (solid line). Figure is the same as in Publication VI (Reproduced by permission of ECS – Electrochemical Society).

A lot of examples in literature can be found in which the quenching and loading is done before isothemal gettering[13,39,45] although the effect of this RT step on the final gettering efficiency is not generally considered in the analysis. Here, we analyze the experimental results of Aoki et al.[39] shown by symbols in Fig. 8. Aoki et al.[39] used two different densities of oxide precipitates named as IG and long term IG samples. The long term IG samples had a longer nucleation time for the oxide precipitates which is why the greater density of the oxide precipitates is used in that case in the simulation.

The experimental results shown in Fig. 8 b) seems to be disagreement with results shown in Fig. 2, i.e. there should not be any gettering at 670 °C at a contamination level of 4×10^{12} cm^{-3}. Actually, the explanation for this disagreement is rather simple: iron precipitates nucleated during the RT-step and the gettering, i.e. growth of iron precipitates, occurs at 670 °C. This kind of behavior is in agreement with the simulations (as shown in Fig. 8) and with the experimentally observed results (Fig. 7 and Publication III).

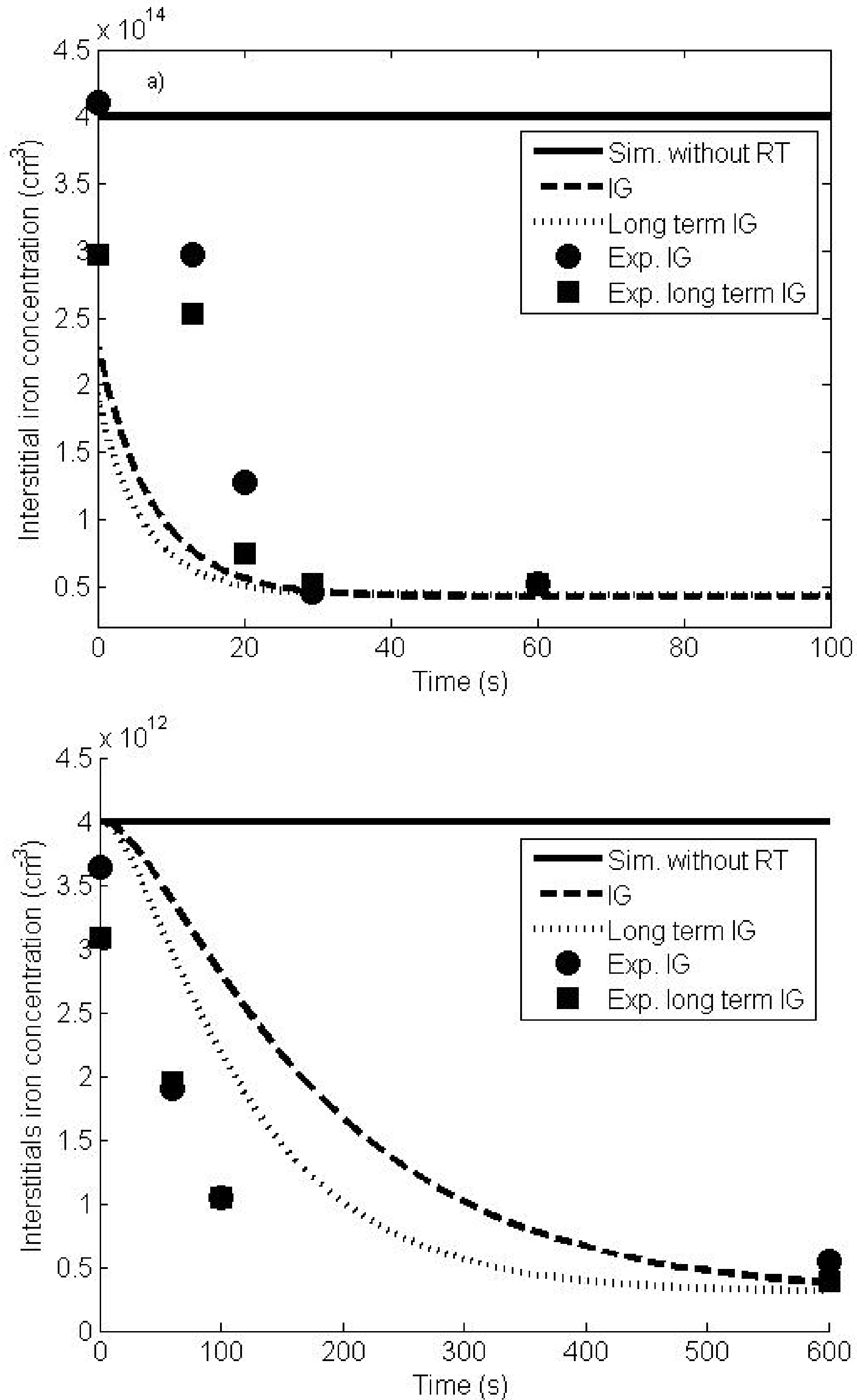

FIG. 8. The interstitial iron concentration (in the DZ) dependence on annealing time: a) at 900 ^{o}C the initial iron concentration is 4×10^{14} cm^{-3} and b) at 670 ^{o}C the initial iron concentration is 4×10^{12} cm^{-3}. The squares and circles are experimental results of Aoki et al..[39] The simulated results without the RT-step (solid line) and with the RT-step (Dashed and dotted lines). In the simulations the density of oxide precipitates and radius is set to, 5×10^{9} cm^{-3} and 180 nm or 5×10^{10} cm^{-3} and 80 nm, in IG samples or in long term IG samples, respectively. The DZ is 40 μm.

3.2.4 Gettering dependence on size and density of oxide precipitates

It was found that at a constant initial iron concentration, the model predicts the $N_{ox}r_{ox}^2$-dependency in gettering efficiency when nucleation limits the gettering efficiency. The results of the model can be easily explained as nucleation produces the density of the effective gettering site N_{eff}~$N_{ox}r_{ox}$ (Eqs. (8) and (15)) and the final gettering efficiency after growth of iron precipitates depends on $N_{eff}\, r_{ox}$-product as

$$\mathrm{GE} = 100 \times \left[1 - \exp\left(-t_G 4\pi D N_{eff} r_{ox}\right)\right] \ , \qquad (25)$$

where t_G is the length of the growth anneal. The results of the simulation example, 30 min gettering anneal at 670 °C after RT-step, is shown in Fig. 9. Clearly, the gettering efficiency depends on total surface of oxide precipitates and Eq. (25) gives nearly the same gettering efficiency as the simulation.

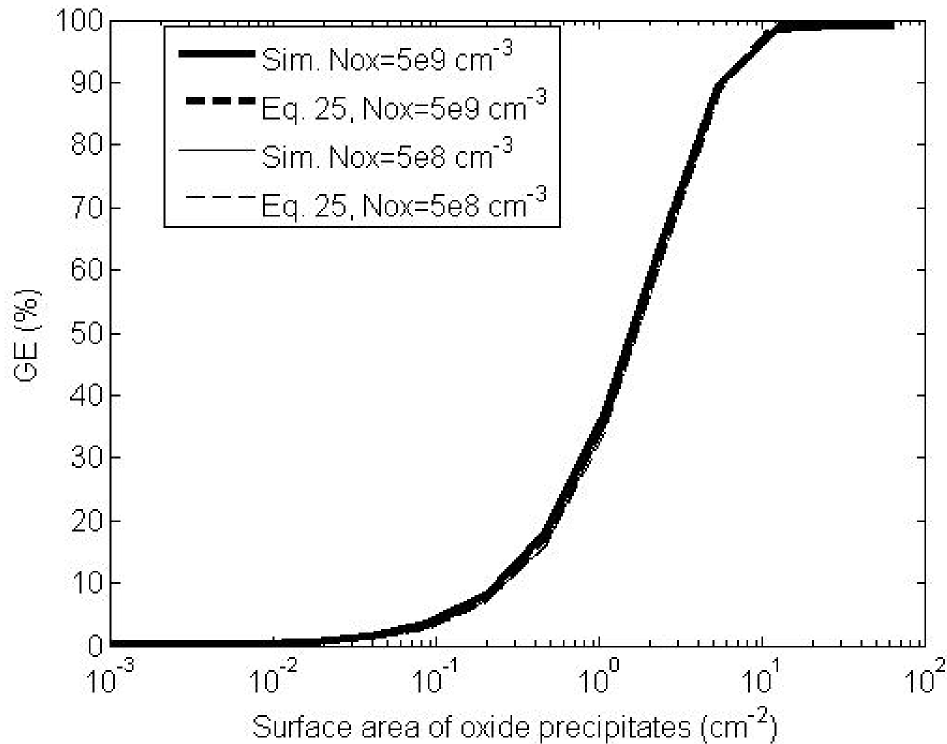

FIG. 9. Comparison of simulation results and Eq. (25). In Eq. (25) N_{eff} is taken from the simulation results of the RT-step.

Ogushi et al.[45] reported that the gettering efficiency of iron correlates with the total volume of oxide precipitates which is clearly in disagreement with the results of Takashit et al.[28], however, the contamination level and gettering technique were different. Ogushi et al.[45] used an initial contamination level of about 1×10^{12} cm^{-3} and the gettering was done by a long isothermal anneal after quenching to room temperature. This means that the final gettering

efficiency was determined by iron nucleation during the room temperature step. From the modeling perspective this might indicate that the iron precipitation under some supersaturation (or/and at small iron precipitate sizes) is reaction limited. In our case this means that the dissolution and growth rate are proportional to the square of the oxide precipitate radius[46], which, at the maximum, leads to $N_{ox}r_{ox}^4$ dependency in the gettering efficiency when both nucleation and growth are reaction limited.

Basically, the model could also be adjusted so that the number of possible gettering sites in the beginning of the simulation is $[5\times10^{13}\text{cm}^{-2}]\ r_{ox}^2N_{ox}$ and P_1=1, then the gettering efficiency should depend on $N_{ox}r_{ox}^4$. However, in this case at high supersaturation the density of effective gettering sites could be larger than the density of oxide precipitates and growth (dissolution) rates should be modified to ensure that gettering is not faster than predicted by Ham's law.

Still, it was shown in Publication V by comparing experimental results of Takashi et. al. to our simulations that the model captures the effect of the oxide precipitate radius and density on the iron gettering reasonable well.

3.2.5 Thermal stability of gettering sites

The thermal stability of internally gettered iron has been studied by many authors[30,37,47] and it is known that after sufficient annealing the iron will be completely dissolved. Zhang et al.[37] studied the dissolution process in more detail by using wafers which had an oxide precipitate density of 5×10^9 cm^{-3} and the average radius was estimated to be 88 nm. They contaminated samples by iron to a level of about 1×10^{14} cm^{-3} at 950 ºC. After that, the gettering was done by cooling samples at 14 ºC/min to 700 ºC. The samples were kept at 700 ºC for 30 min and then cooled to 450 ºC at a rate of about 8 ºC/min. The final ungettered iron concentration measured after that was 5×10^{10} cm^{-3}. The iron dissolution was then studied by annealing samples between 750-900 ºC for different times.

The simulation of the above described gettering treatment gives the remaining dissolved iron concentration of 1.9×10^{11} cm^{-3} which is reasonable close to the measured 5×10^{10} cm^{-3}. In Fig. 10 is shown the simulated and measured results of the dissolution of gettered iron at 800 ºC. The simulated and measured results, especially the timescale of dissolution, agree quite well. Actually, dissolution time constants calculated by using an effective density of about 1×10^8 cm^{-3}, which is a simulation result, deviated significantly only at 750 ºC from experimentally[37] determined dissolution time constants. This means that the simulation of iron precipitation and dissolution can be performed consistently using the same model with no need to use a dissolution barrier proposed by Zhang et al.[37] as both the precipitation and the dissolution time constants are inversely proportional to the density of the effective gettering site.

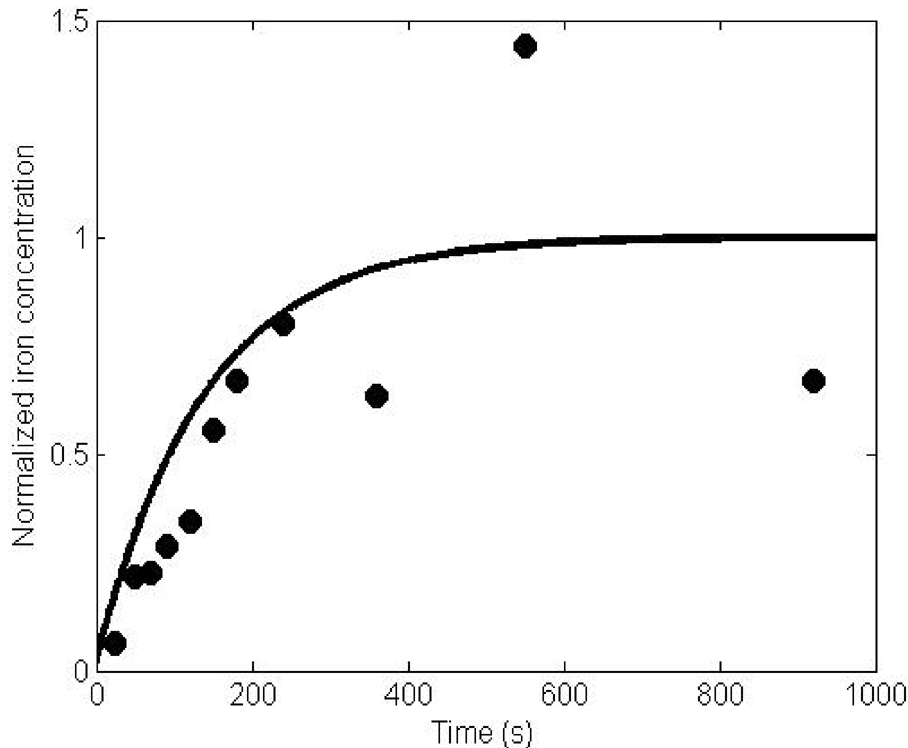

FIG. 10. The simulated (line) and experimental results (circle) dissolved iron concentration versus time in dissolution anneal at 800 ºC. The experimental results are from reference 37.

.

3.3 Gettering in process

In literature the effect of IG on device parameters or yield[5,48-50] and on iron concentrations[51-54] close to the surface after different simulated process steps (including also different starting materials) is studied quite a lot in order to evaluate the gettering capability of bulk defects at certain stages of the process. It is common in these studies that the gettering capability is considered only as point of view of existence of bulk defects. This means that it is assumed that the gettering efficiency should be good whenever there exists a lot of (>10^9 cm^{-3}) bulk defects.

Now, it is clear that the existence of oxide precipitates and related defects do not guarantee efficient gettering. To achieve efficient gettering the iron precipitates must be nucleated at a sufficiently number of bulk defects. This nucleation strongly depends on the contamination level. The effect of the contamination level is not generally considered in studies presented in literature and we can actually divide findings into two categories: no gettering at any bulk defect density in low contamination studies[5,48-51] (iron concentration well below 1×10^{13} cm^{-3}) and increasing gettering with increasing bulk defect density in high contamination studies[52-54] (iron concentration well above 1×10^{13} cm^{-3}). These are reasonable results, if we consider e.g. the simulation results in Fig. 3 and the experimental results of Publications I and II, as in these studies gettering is also done by cooling the wafers from high temperatures.

We know that at low contamination levels iron precipitates can be formed by low-high-treatment; where low can simply be a ramp to room temperature, as shown in Publications III,

IV and VI, and by analysis of the results of Aoki et al.[39]. However, the iron precipitates dissolve at high temperatures, and total dissolving is expected in standard furnace annealing, if the solubility at the processing temperature is higher than the contamination level. Total dissolving obviously removes gettering capability but, on the other hand, it also removes iron precipitates from the device layer. The gettering capability is not necessarily removed even in the case that the solubility at the processing temperature is higher than the contamination level, if processing times are very short, like in rapid thermal anneals (RTA), as the iron precipitates are dissolved only partially. Obviously, the dissolution of iron precipitates must be simulated correctly, if the gettering capability in process steps after RTA is concerned.

Istratov et al.[8] pointed out that iron becomes detrimental when it agglomerates in relatively weakly doped areas, or form precipitates in the device layer which also penetrates into weakly doped regions or at the gate oxide interface. We propose that the optimal place for "low-high" gettering is after the last process step in which the solubility is higher than the contamination level, i.e. after the last step in which complete dissolution of iron precipitates (in the device layer and in bulk) occurs. Here, we assume that device performance is mainly determined by the final concentration of metal precipitates and dissolved iron concentration in the device layer. E.g. at a contamination level of 5e12 cm^{-3}, low-high should be after the last process step in which the temperature is higher than 790˚C.

The interesting question is: what is the effect of lattice defects formed by metal precipitation on the final device performance? This means, that although the iron precipitates itself may dissolve, the secondary defect may still exist and have a significant impact on the device. It is also possible that secondary defects also make the next nucleation of iron precipitates easier. This kind of effect was not observed during our experiments although some of the samples were re-used after successful gettering and dissolution anneals.

In publication V we propose that the iron precipitation model can be easily extended to copper and nickel. The argument for this is very simple; generally in all precipitation growth of precipitates can occur only after nucleation, which is included in the proposed model. In practical gettering, there is still a difference between copper, nickel and iron. In the case of copper and nickel the main task is to prevent precipitation in a device layer (wafer surface). In case of iron also the dissolved concentration must be removed from a device layer due to its high electrical activity. Actually, this is the reason why iron gettering is much harder than gettering nickel and copper.

4 Conclusions

In this thesis the heterogeneous iron precipitation was studied in silicon using oxide precipitates and related defects as precipitation sites. The iron concentration was monitored using Deep Level Transient Spectroscopy (DLTS), Surface Photo Voltage SPV and Microwave Photoconductive Decay (μ-PCD). Part of the work was to calibrate the lifetime methods, μ-PCD and SPV, by direct DLTS measurement and find out the applicability of lifetime methods for iron detection in internally gettered silicon wafers. In addition, Transmission Electron Microscopy (TEM) analyses were performed to determine the size of oxide precipitates and defect etching (Wrigth etch) was used to determine the density of oxide precipitates.

The contamination level has a major impact on the gettering efficiency as a high supersaturation, ~0.34 eV, is needed before significant nucleation of iron precipitates can occur. The internal gettering of iron at low levels of initial iron concentration ($<1\times10^{12}$ cm^{-3}) is practically impossible just by cooling. The low temperature nucleation anneal is needed to induce a significant number of iron precipitates which further grow and getter iron at higher temperatures. For optimal IG the proper combination of nucleation and growth steps of iron precipitates must be found. The nucleation step can be a fast ramp, even quenching, and this effect was not usually taken into account in past experiments and analysis of iron precipitation. In practice the growth step can be in a temperature range, in which a competitive gettering by a heavily doped device layer is significant. In this case the particular advantage of IG is the reduction of the iron precipitate density in the device layer. Also the increased solubility in the device layer reduces, and may even completely prevent, the iron precipitation in the device layer.

The optimal place for two step gettering is after the last high temperature anneal in which all iron precipitates are dissolved, if it is assumed that device performance is mainly determined by the final concentration of metal precipitates and dissolved iron concentration in the device layer. In the future, it would be interesting to study the effect of the optimized internal gettering in a real device process. Are there really some benefits of placing iron in bulk defects at the end of the process or is this masked by the detrimental effect of the precipitation-dissolution cycles?

A model is presented for the heterogeneous precipitation of iron to oxygen-related defects in silicon during thermal processing. In the model we use special growth and dissolution rates, which are inserted into a set of modified CRE or into FPE, to simulate time evolution of iron precipitates. This approach allows us to calculate the size distribution of iron precipitates and the residual iron concentration. By comparing the simulated results with experimental ones, our own or taken from literature, it is proved that this model can be used to estimate the internal gettering efficiency of iron under a variety of processing conditions. The presented model extends straightforwardly to any other precipitation gettering technique (or metal) by finding proper growth and dissolution rates, although in this thesis the model is only applied to internal gettering of iron precipitation. In the future, it would be interesting to use the model and optimize the size distribution of iron precipitates in a multicrystalline silicon solar cell process.

References

[1] A.A. Istratov, H. Hieslmaier and E. R. Weber, Physica B **273-274**, 412 (1999).

[2] A.A. Istratov, H. Hieslmair and E. R. Weber, Appl. Phys. A **69**, 13 (1999).

[3] A.A. Istratov, H. Hieslmair and E. R. Weber, Appl. Phys. A **70**, 489 (2000).

[4] S. M. Myers, M. Seibt, and W. Schröter, J. Appl. Phys. 88, 3795 (2000).

[5] F. Bialas, R. Winkler, and H. Dietrich, Microelectron. Eng. **56**, 157 (2001).

[6] M. J. Binns, S. Bertolini, R. Wise, D. J. Myers, and T. A. McKenna, 9th Int Symp. Silicon Materials Science & Technology, Philadelphia, May 12-17, 2002.

[7] R. Hoelzl, L. Fabry, K.jJ. Range, R. Wahlich, G. Kissinger, Microelectron. Eng. **56**, 153 (2001).

[8] A. A. Istratov, W. Huber, and E. R. Weber, J. Electrochem. Soc. **150**, G244 (2003).

[9] H. Kohno, H. Hieslmaier, A. A. Istratov, and E. R. Weber, *Appl. Phys. Lett.* **76**, 2734 (2000).

[10] A. A. Istratov, T. Bunassisi, R. J. McDonald, A. R. Smith, R. Schindler, J. A. Rand, J. P. Kalejs, and E. R. Weber, J. Appl. Phys. **94**, 6552 (2003).

[11] T. Buonassisi, A. A. Istratov, M. Heuer, M. A. Marcus, R. Jonczyk, J. Isenberg, B. Lai, Z. Cai, S. Heald, W. Warta, R. Schindler, G. Willeke, and E. R. Weber, J. Appl. Phys. **97**, 074901 (2005).

[12] T. Buonassisi, A. A. Istratov, S. Peters, C.Ballif, J. Isenberg, S. Riepe, W. Warta, R. Schindler, G. Willeke, B. Lai, Z. Cai, and E. R. Weber, J. Appl. Phys. **97**, 074901 (2005).

[13] H. Hieslmair, A. A. Istratov, S. A. McHugo, C. Flink, T. Heiser, and E. R. Weber, *Appl. Phys. Lett.* **72**, 1460 (1998).

[14] H. Hieslmair, S. Balasubramanian, A. A. Istratov, and E. R. Weber, *Semicond. Sci. Technol.* ***16***, 567 (2001).

[15] A. L. Smith, K. Wada, and L. C. Kimerling, *J. Electrochem. Soc*. **147**, 1154 (2000).

[16] T. Y. Tan, R. Gafiteanu, S. M. Joshi, and U. Gösele, in *Semiconductor silicon 1998*, edited by H. Huff, U. Gösele, and H. Tsuya (The Electrochemical Society, Pennington, NJ, 1998), p. 1050.

[17] H. Hieslmaier, A. A. Istratov and E. R. Weber, *Semicond. Sci. Technol.* **13**, 1401 (1998).

[18] K. Nakamura and J. Tomioka, in Proceedings of The Electrochemical Society Spring 2006 Meeting, Denver, Colorado, edited by H. Huff, L. Fabry, D. Gilles, U. Goesele, T. Hattori, W. Huber, S. Ikeda, H. Iwai, P. Packan, H. Richter, M. Rodder, E. Weber, R. Wise, (The Electrochemical Society, Pennington, NJ, 2006), pp.275-286.

[19] P. Geranzani, M. Pagani, C. Pello, and G. Borionetti, *Solid State Phen.* **82-84**, 381 (2002).

[20] F. S. Ham, *J. Phys. Chem. Solids* **6**, 335 (1958).

[21] D. Gilles, E. R. Weber, and S. Hahn, *Phys. Rev. Lett*. **64**, 196 (1990).

[22] R. J. Falster, G. R. Fisher, and G. Ferrero, Appl. Phys. Lett. **59**, 809 (1991).

[23] R. Falster, in *Crystalline Defects and Contamination: Their impact and Control in Device Manufacturing,* Proceeding of the Satellite Symposium to ESSDERC 93 Grenoble, France, edited by B. O. Kolbesen, C. Claeys, P. Stallhofer, and F. Tardif (The Electrochemical Society, Pennington, NJ, 1993), pp. 149-169.

[24] S. A. Mchugo, R. J. McDonald, A. R. Smith, D. L. Hurley, and E. R. Weber, Appl. Phys. Lett. **73**, 1424 (1998).

[25] H. Hieslmaier, A. A. Istratov, C. Flink, S. A. Mchugo and E. R. Weber, Physica B **273-274**, 441 (1999).

[26] D. Kashchiev, *Nucleation: basic theory with applications*, (Butterworth-Heinemann, Oxford, 2000), p. 77.

[27] S. T. Dunham, Appl. Phys. Lett. **63**, 464 (1993).

[28] H. Takahashi, H. Yamada-Kaneta, and M. Suezawa, Jpn. J. Appl. Phys. **37**, 1689 (1998).

[29] J. Vanhellemont and C. Claeys, Mater. Sci. Forum **38**, 171 (1989).

[30] S. A. McHugo, E. R. Weber, M. Mizuno and F. G. Kirscht, Appl. Phys. Lett. **66**, 2840 (1995).

[31] A. Mesli, T. Heiser, N. Amroun, and P. Siffert, *Appl. Phys. Lett.* **57** 1898 (1990).

[32] S. Kobayashi, J. Crystal Growth **174**, 163 (1997).

[33] J. S. Chang, and G. Cooper, J. Comp. Phys. **6**, 1 (1970).

[34] H. Takeno, T. Otogawa, and Y. Kitaqawara, J. Electrochem. Soc. **144**, 4340 (1997).

[35] H. Lemke, Phys. Stat. Sol. A **76**, 223 (1983).

[36] L. C. Kimerling and J. L. Benton, Physica **116B,** 297 (1983).

[37] P. Zhang, H. Väinölä, A. A. Istratov, and E. R. Weber, Physica B **340-342**, 1050 (2003).

[38] M. Porrini and P. Tessariol, Mater. Sci. Eng. **B73**, 244 (2000).

[39] M. Aoki, A. Hara, and A. Ohsawa, J. Appl. Phys. **72**, 895 (1992).

[40] H. Hieslmaier, A. A. Istratov, T. Heiser, and E. R. Weber, J. App. Phys. **84**, 713 (1998).

[41] R. A. Brown, O. Kononchuk , and G. A. Rozgonyi, Nucl. Instr. And Meth. in Phys. Res. B **148**, 322 (1999).

[42] K. Graff, *Metal Impurities in Silicon-Device Fabrication,* (Springer-Verlag, Berlin, 2000), p. 22

[43] A. Borghesi, B. Pivac, A. Sassella, and A. Stella, J. Appl. Phys. **77**, 4169 (1995).

[44] M. Palokangas, *Characterization of internal gettering of iron in silicon by DLTS,* Master's Thesis, Helsinki University of Technology (2002).

[45] S. Ogushi, S. Sadamitsu, K. Marsden, Y. Koike and M. Sano, Jpn. J. Appl. Phys. **36**, 6601 (1997).

[46] J. M. Hwang, and D. K. Schroder, J. Appl. Phys. **59**, 2476 (1986).

[47] M. Aoki and A. Hara, J. Appl. Phys. **74**, 1440 (1993).

[48] R. W. Gregor, and W. H. Stinebaugh, J. Appl. Phys. **64**, 2079 (1988).

[49] G. F. Ceroflini, and M. L. Polignano, J. Appl. Phys. **55**, 579 (1984).

[50] M. L. Polignano, G. F. Cerofolini, H. Bender, and C. Clayes, J. Appl. Phys. **64**, 869 (1988).

[51] G. Kissinger, J. Vanhellemont,G. Morgensten, M. Blietz, K. Tittelbach-Helmrich, G. Obermeier, and R. Wahlich, in *Defects in Silicon III,* Electrochemical Society Proceedings, Vol. 99-1, 1999, , edited by W. M. Bullis, W. Lin, P. Wagner, (The Electrochemical Society, Pennington, NJ, 1999), pp. 268-279.

[52] J. G. Park, G. S. Lee, J. S. Lee, K. Kurita, and H. Furuya, Material Sciene and Engineering B **134**, 249 (2006).

[53] J. G. Park, K. Kurita, G. S. Lee, S. A. Lee, and H. Furuya, Microelectron. Eng. **66**, 247 (2003).

[54] M. Shabani, Y. Shiina, and Y. Shimanuki, Solid State Phen. **95-96**, 539 (2004).

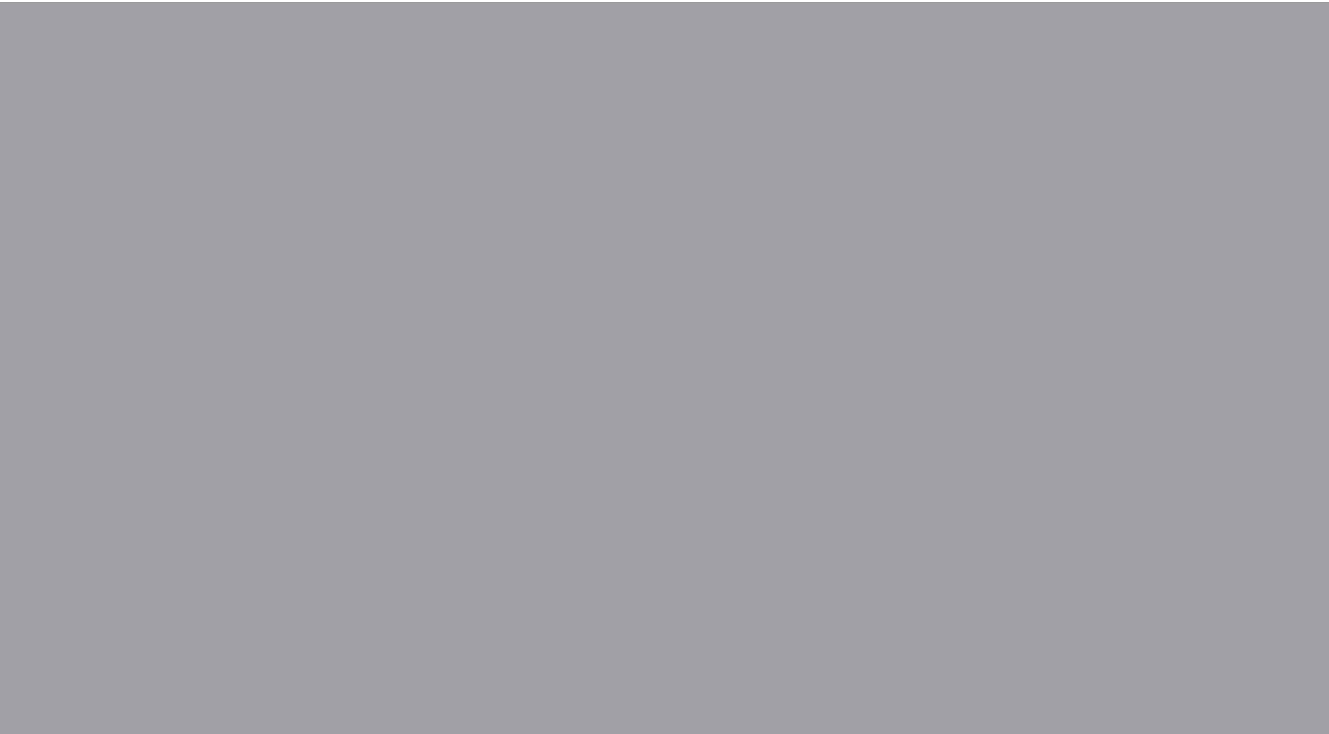

ISBN 978-951-22-8683-6
ISBN 978-951-22-8684-3 (PDF)
ISSN 1795-2239
ISSN 1795-4584 (PDF)